

Numerical Investigation of Velocity Map of Outward Electrons Penetrating in Helical Magnetic Surfaces

Kazutaka NAKAMURA¹⁾, Haruhiko HIMURA¹⁾, Mitsutaka ISOBE²⁾,
Akio SANPEI¹⁾, and Sadao MASAMUNE¹⁾

¹⁾*Kyoto Institute of Technology, Department of Electronics, Matsugasaki, Kyoto 606-8585, Japan*

²⁾*National Institute for Fusion Science, Gifu 509-5292, Japan*

(Received: 3 September 2008 / Accepted: 5 January 2009)

In order to investigate the formation process of helical nonneutral plasmas, we numerically perform a mapping of velocity space of outward electrons whose orbits extend to inward part of closed helical vacuum magnetic region of the Compact Helical System machine. Contrary to the experimental observation, the penetrating electrons exist in quite narrow region on the velocity map, which are the vicinities of initial pitch angle $\sim 90^\circ$.

Keywords: Helical nonneutral plasmas, Velocity mapping, Helically trapped particle, Electron injection, stochastic magnetic region

1. Introduction

Research on nonneutral plasmas confined on toroidal magnetic surfaces has been intensively conducted in recent years [1, 2]. Despite the closed magnetic surfaces, no break-up of those is required when the plasmas are produced. In experiments on devices of the Compact Helical System (CHS) [3] and the Heliotron J [4], an electron-gun (hereafter, e-gun) has been installed in the stochastic (or ergodic) magnetic region (SMR) [5] surrounding the last closed flux surface (LCFS) and just ejected thermal electrons in the SMR. Then, within the order of $10 \mu\text{s}$ after the injection, those have penetrated deeply in the helical magnetic surfaces (HMS), spread rapidly in the whole of the closed surfaces, and finally formed a helical nonneutral plasma there [6].

Regarding the mechanism of the inward penetration of electrons, recent three dimensional orbit calculations including two experimental findings have finally outputted some outward orbits that extend to inward part of closed helical vacuum magnetic region [7]. Data have clearly shown that the pitch angle of electron injected into the stochastic magnetic region is scattered considerably due to the presence of self space potential ϕ_s . Eventually, the injected electron turns to be a helically trapped particle [8, 9], and start an inward movement along one of the $|B_{min}|$ contours [3, 7, 10]. Once penetrating deeply, the electron can never escape from the LCFS because the negative ϕ_s acts as a potential barrier.

However, in the calculations explained above, only two orbits extending to inward part of closed HMS region were discovered. Obviously, this calls for a survey of the outward orbit with changing its initial conditions, especially the pitch angle. In this paper, we report a velocity map of electrons injected into the SMR.

Surprisingly, the penetrating electrons exist only in a narrow region on the velocity map, which pitch angle $\arctan(v_\perp/v_\parallel)$ is the range between $\sim 75^\circ$ and $\sim 105^\circ$. In Sec. 2, the model employed in this computation is briefly explained. Data obtained from the calculation and the velocity map are given in Sec. 3. Finally, a summary is given in Sec. 4.

2. Calculation Model

Since experiments have been conducted on CHS, we have used magnetic field structure of the machine. In addition, as mentioned in Sec. 1, two experimental findings have been recently taken into account in the numerical code. Since those are already described in Ref. [6], we will briefly review them in the following for reader's convenience.

Firstly, in the SMR, considerable ϕ_s (down to

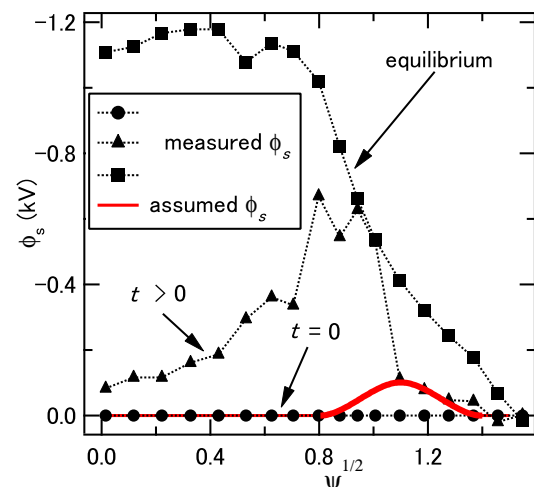


Fig. 1 The modeled self electrostatic potential ϕ_s in the stochastic magnetic region (SMR) and its vicinity. The profile is determined from the measured data.

author's e-mail: nakamu6t@nuclear.es.kit.ac.jp

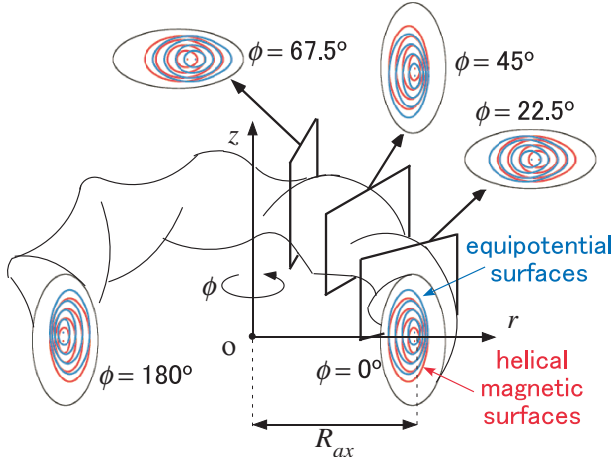


Fig. 2 A schematic drawing of three-dimensional structure of the Compact Helical System (CHS) chamber wall with projections of helical magnetic surfaces (HMS) and equipotential surfaces (EPS).

~ -100 V) has been observed in experiments. This is because lines of force in the SMR are chaotic, the connection lengths of those to the grounded chamber wall are very long. Therefore, thermal electrons injected from the e-gun are confined there. The whole profile of ϕ_s in the SMR has been model from the experimental data. The solid curve in Fig. 1 shows the assumed ϕ_s , while the plotted data are typical time evolution of ϕ_s measured in experiments. Then, we have assumed symmetrical equipotential surfaces (EPS) of ϕ_s that are exactly the same as the elliptical magnetic surfaces described in Fig. 2, except that the center of the EPS is shifted from that of the HMS, as will be explained below.

Secondly, recent experimental works have revealed [1] that the value of ϕ_s (equivalently, the electron density n_e) is not constant on magnetic surfaces. These results mean that the EPS are never coincided with the HMS. Inferring by the obtained data in CHS experiments, the EPS seems to shift about 2 cm for the case of magnetic axis $R_{ax} = 101.6$ cm and $B = 0.9$ kG. As explained, the SMR acts as quasi-confinement region so that such displacement of the EPS would be in part held even in the SMR, although no perfect closed HMS exist there. Therefore, in this calculation, we assume the presence of the shifted EPS which extend to the SMR. Regarding the structure of the EPS in toroidal direction, we have adopted helical symmetry. Defining the cylindrical coordinate as seen in Fig. 2, the coordinates of the center of the shifted EPS can be calculated from the relations of

$$\left. \begin{aligned} r_{eps} &= r_{hms} - 0.02 \times \sin 4\phi \\ z_{eps} &= z_{hms} + 0.02 \times \cos 4\phi \end{aligned} \right\} \quad (1)$$

where ϕ is the toroidal angle and the phase of

4ϕ comes from the toroidal mode number ($m = 8$) of CHS. In Fig. 2, appearances of both EPS and HMS in poloidal cross-sections are also depicted.

3. Orbit Calculations

Orbits of the electrons injected into the SMR have been calculated by solving the equation of motion $\vec{v} = -e(\vec{v} \times \vec{B} + \vec{E})/m$ with the 6th order Runge-Kutta-Verner method in cylindrical coordinates. In calculation, we have varied the initial absolute value of velocity and pitch angle of the e-gun. Other parameters listed below are fixed as follows; the strength of $|\vec{B}|$ at $R_{ax} = 101.6$ cm is 0.9 kG and the injection position of a single electron is at $\psi^{1/2} = 1.0$ on the equatorial plane, where $\psi^{1/2}$ is the normalized minor radius.

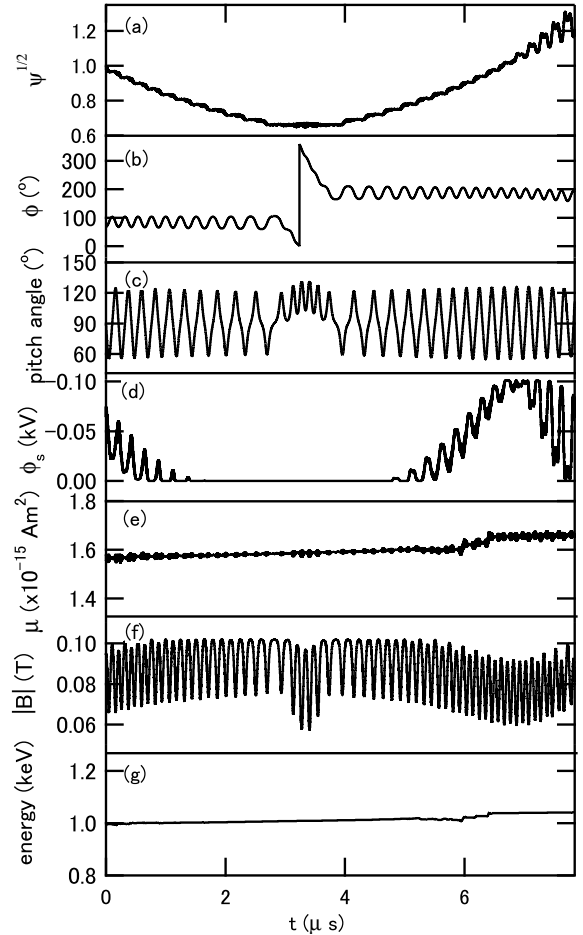


Fig. 3 Time evolutions of (a) normalized position, (b) toroidal angle, (c) pitch angle, (d) electrostatic potential, (e) magnetic moment, (f) magnetic field strength, and (g) total energy of the injected electron, for the case of initial pitch angle $\sim 90^\circ$. It is clearly shown that the injected electron successfully penetrates across the LCFS.

3.1 Penetration orbit

In this subsection, we explain how the injected electron turns to become helically trapped particle and penetrates the HMS, shortly. The detail is described in Ref. 6, readers can refer it. Figure 3 shows the time evolutions of all parameters of the injected electron which penetrates into the CHS, for the case of initial pitch angle $\sim 90^\circ$. In this case, the injected electron become helically trapped particle (HTE), initially.

The position of the injected electron can be understood from Fig. 3 (a) in which the time evolution of the normalized radial coordinate $\psi^{1/2}$ of the particle is shown. As clearly recognized, the electron penetration happens at $t \sim 0 \mu\text{s}$.

For the period of $0 < t < 7 \mu\text{s}$, the electron is completely trapped in bottoms of helical ripples, which is also recognized from Figs. 3 (b) and (c). Since no ϕ_s exists in the inner part of the HMS, the magnetic moment μ of the electron is preserved there (see also Figs. 3 (d) and (e)). Then, the HTE travels inwardly along $\text{mod}|B_{\min}|$ contours where the strength of \vec{B} is weaker compared to the neighborhood region on each magnetic surface, which is just the same as the motion of HTE of neutral plasmas [5]. In this calculation, as long as ϕ_s is independent of time, total energy is conserved, as seen from Fig.3 (g).

After passing through the closest point from the magnetic axis R_{ax} at $t \sim 6 \mu\text{s}$, the HTE travels outwardly towards the LCFS. The HTE is lost across the LCFS in this case, but then negative ϕ_s increases (see also Fig.1), it acts as a potential barrier against the outward drifting particle [7]. This results in the trapping of the HTE in the HMS.

3.2 Loss orbit

On the other hand, the injected electron does not always penetrate across the LCFS. This can be understood from Fig. 4. Data in Fig. 4 are outputted from an electron launched from the e-gun with an initial pitch angle $\sim 10^\circ$. The injected electron sticks around the LCFS, as shown in Fig. 4 (a). For this case, as recognized from Fig. 4 (b), the electron rotates the torus at all times from $t = 0 \mu\text{s}$ to the calculation end (at $t \sim 12.5 \mu\text{s}$). No transition electron or helically trapped one can be found for this case at all. The injected electron has been in the state of passing electron, all the time.

The above result can be inferred from the time history of the pitch angle shown in Fig. 4 (c). Although the injected electron always stays in the region of finite ϕ_s as seen in Fig. 4 (d), the value of pitch angle varies only in the range between $\sim 8^\circ$ and $\sim 14^\circ$.

Actually, the variation is very smaller than that of the penetration orbit, as already shown in Fig. 3 (c).

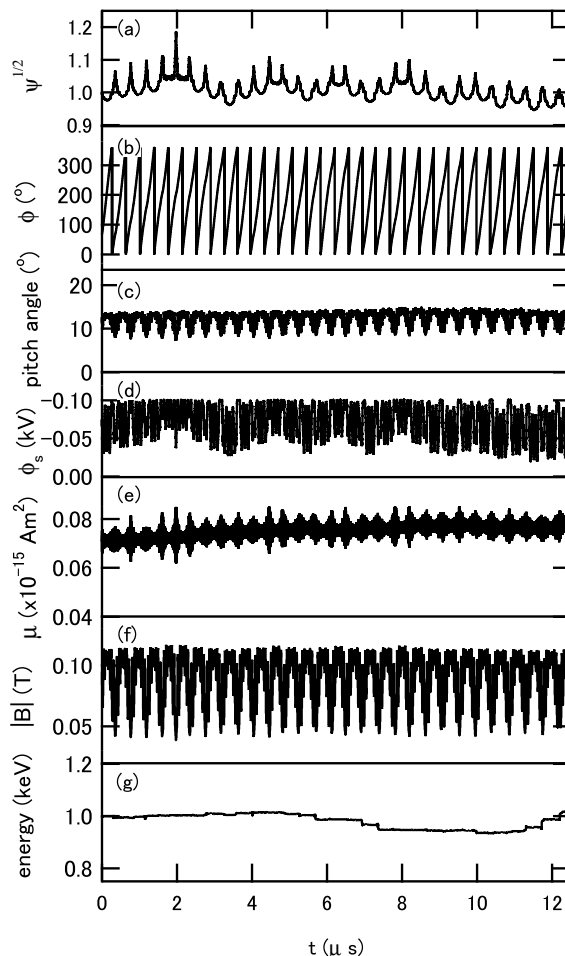


Fig. 4 Time evolutions of all parameters for the case of initial pitch angle $\sim 10^\circ$. Parameters here are the same as those in Fig. 3, for reader's convenience. As recognized, no penetration of the injected electron occurs for this case. The electron has been always in the state of passing particle in the vicinity of LCFS.

In fact, no considerable change in the pitch angle is caused for this case. Consequently, no penetration of the injected electron occurs, because the transition to a HTE is never happened.

3.3 Velocity mapping

As explained above, the inward penetration across the LCFS has depended on whether the transition to a HTE occurs or not, and moreover, the transition is affected much by the initial pitch angle of the injected electrons. Thus, we have performed a mapping of the initial pitch angle with changing its kinetic energy V_{acc} (equivalently, beam energy in experiments): $V_{acc} = -0.8 \text{ kV}$.

Figure 5 shows the velocity map for electrons ejected from the e-gun. Orbit calculations are conducted up to $12.5 \mu\text{s}$. Two symbols (\bullet and \times) on the map represent successful- and in-successful penetra-

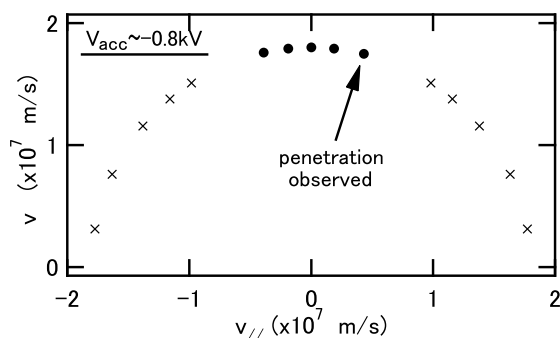


Fig. 5 The velocity map for the electron launched from the e-gun placed at the point $(r, \phi, z) = (1.0325, 67.5, 0.14)$. The penetration happens (indicated by \bullet) when the value of initial pitch angle exists in the range between $\sim 75^\circ$ and $\sim 105^\circ$, while does not for all values indicated by \times .

tion, respectively. As recognized from black circles, several areas are found on the map for the successful penetration for the case of $V_{acc} = -0.8$ kV, which are the vicinities of pitch angle between $\sim 75^\circ$ and $\sim 105^\circ$. The result of initial pitch angle $= 80^\circ$ seems to be consistent with the experimental observation [11]. In fact, considerable ϕ_s in the HMS have been quickly formed even with a small beam current I_b of the injected electrons (see also Fig. 2 in Ref. [11]). However, in the past experiments, such a quick formation of ϕ_s was also observed for initial pitch angle $\sim 150^\circ$, while no penetration (inevitably, no formation of ϕ_s in the HMS) happens at all in the computation shown in Fig. 5. In fact, in the experiments, finite ϕ_s were always measured in the HMS as long as $I_b > \sim 5$ mA, regardless of the pitch angle. This discrepancy is still under investigation, however possibly due to the assumption of completely static ϕ_s in computation which is never the case in actual experiments.

Since the electron penetration has occurred with lower values of $|V_{acc}|$ (see also Fig. 1 in Ref. [11]), we will examine other cases of $|V_{acc}| < 0.8$ kV.

4. Summary

In order to investigate the formation process of helical nonneutral plasmas, we have numerically performed a mapping of velocity space of outward electrons whose orbits extend to inward part of closed helical vacuum magnetic region of the Compact Helical System machine. In calculations presented here, the magnetic axis R_{ax} is fixed to be $R_{ax} = 101.6$ cm and the magnetic field strength is $B = 0.9$ kG. Those are exactly the same as those in the settings of actual experiments. And, in this computation, electron full orbits are solved using the 6th Runge-Kutta method to include the effect of Larmor motion.

Data show that the penetrating electrons having

the initial kinetic energy of 0.8 keV exist in quite narrow region on the velocity map, which are the vicinities of initial pitch angle $\sim 90^\circ$. In fact, the result of initial pitch angle between $\sim 75^\circ$ and $\sim 105^\circ$ seems to be consistent with the experimental observation. However, no penetration is observed in computation with other values of initial pitch angle, while certainly occurs in experiments. This discrepancy is still under investigation, however possibly due to the assumption of completely static ϕ_s in computation.

Acknowledgment

The authors are grateful to Drs. A. Shimizu, K. Matsuoka, and S. Okamura of NIFS for their continuous encouragements. This work is performed under the auspices of the NIFS CHS Research Collaboration, No. NIFS07KZPH002.

- [1] H. Himura *et al.*, Phys. Plasmas **14**, 022507 (2007).
- [2] M. Hahm *et al.*, Phys. Plasmas **15**, 020701 (2008).
- [3] S. Okamura *et al.*, Nucl. Fusion **39**, 1337 (1999).
- [4] T. Obiki *et al.*, Plasma Phys. Control. Fusion **42** 1151 (2000).
- [5] M. Isobe *et al.* Nucl. Fusion **41**, 1273 (2001).
- [6] H. Himura *et al.* Phys. Plasmas **11**, 492 (2004).
- [7] K. Nakamura *et al.*, submitted to Phys. Plasmas (2008).
- [8] M. H. Redi *et al.* Phys. Plasmas **6**, 3509 (1999).
- [9] A. Shishkin *et al.* Nucl. Fusion **47**, 800 (2007).
- [10] T. Watanabe *et al.* Nucl. Fusion **46**, 291 (2006).
- [11] H. Himura *et al.*, J. Plasma Fusion Res. SERIES **6**, 756 (2004).